Observational evidence of the southward transport of water masses in the Indian sector of the Southern Ocean

Racheal Chacko*, Nuncio Murukesh, Jenson V. George and N. Anilkumar

National Centre for Antarctic and Ocean Research, Headland Sada, Vasco-da-gama, Goa 403 804, India

The southward transport of water masses in the Indian sector of the Southern Ocean (SO) is compared using the hydrographic data collected during the austral summer of 2010 and 2011. It has been found that subtropical surface water (STSW) underwent maximum southward displacement during the study period. The southward extent of STSW was at 45°S during 2011, but was restricted to 42°S during 2010. During 2011, three eddies were identified along the cruise track, whereas during 2010 eddies were absent. Satellite sea-level anomaly showed that these eddies were associated with the highly unstable Agulhas Return Current (ARC). The present study shows that STSW is transported along the peripheries of these eddies during 2011. There are indications of transport of mode water as well, but this is not resolved in the present study. Analysis of eddy kinetic energy shows a positive linear decadal trend; also, peak eddy lagged the southern annular mode by a year. This indicates that though the eddies may act locally, they are linked to the large-scale variability in the southern hemisphere.

Keywords: Eddy kinetic energy, oceanic fronts, subtropical surface water, water masses.

THE Southern Ocean (SO) is a key player in the Earth's climate for its importance in the global ocean circulation and water mass formation, inter-basin connections, and air–sea exchanges of heat, freshwater, and tracer gases[1]. The SO is characterized by a wide spectrum of variability. The high frequency variability largely arises from the wind-driven ocean variability[2–4]. Low frequency variability of inter-decadal timescales also occurs in the SO and to an extent depends on the mesoscale eddies[5], suggesting the role of intrinsic variability in the decadal variability[6]. The eddy kinetic energy (EKE; which is a measure of mesoscale activity) in topographically constrained areas in SO and within the Antarctic Circumpolar Current (ACC) is often dependent on changes in wind forcing on inter-annual to inter-decadal timescales largely associated with major climatic modes such as the Southern Annular Mode (SAM) and El Niño/Southern Oscillation (ENSO)[2,7,8]. Model studies reveal that different geographic regions within the SO respond differently. The Pacific sector is characterized by intrinsic disturbances that respond to SAM and ENSO, whereas the Atlantic sector is largely wind-driven. Satellite observations[9], buoy trajectories[10], inertial jet models[11] and hydrographic data[12–14] have revealed that high mesoscale variability in the SO is closely correlated with regions of prominent bottom relief. This variability also correlates closely with either the terminal region of a major western boundary current such as the Agulhas Current, or where the ACC interacts with prominent bottom topography such as in the Drake Passage or at the Crozet and Kerguelen Plateau[12]. Eddies are also an important feature in the SO. In SO, poleward heat flux that regulates the meridional overturning circulation is influenced by mesoscale eddies[15–17]. Recent literature shows that eddies in the Agulhas retroflection entrap subtropical properties like low oxygen and CFC, and transport to the sub Antarctic zone mostly by eddy translation[18].

The southwest Indian sector of SO is characterized by the confluence of warm Agulhas Return Current (ARC) and Subtropical Convergence[13,19]. This region is known for its enhanced primary productivity and water mass formation and high incidence of mesoscale features[20]. The present study was carried out in the southwestern Indian sector of SO during the Indian scientific expedition to the SO in the austral summer of 2010 and 2011. The study has analysed the thermohaline variations in an area characterized by mesoscale disturbances and attempted to understand the role of eddies in the southward water mass transport as well as examine the year-to-year variability in the region using available datasets and to link it with the large-scale variability.

Data and methods

This study was carried out on-board *ORV Sagar Nidhi* during the 4th and 5th Indian Expedition to SO (February 2010 and 2011). A CTD (Sea-Bird Electronics, USA; temperature precision: ±0.001°C, conductivity: ±0.0001 S/m and depth ±0.005% of the full scale) was used to collect

*For correspondence. (e-mail: racheal@ncaor.gov.in)

temperature and salinity profiles of the upper 1000 m water column at 2° intervals along 57°30′E. In addition, dense underway profiling of the upper ocean temperature and salinity was carried out with expendable conductivity–temperature–depth probes (XCTDs; Tsurumi Seiki Company Limited, Japan; type: XCTD-3; terminal depth: 1000 m; temperature/salinity accuracy: ± 0.02°C/ ± 0.03 mS cm^{-1}) at 30 nautical mile (nm) interval and supplemented full-depth CTD stations that were spaced at approximately 120 nm. Generally, three XCTDs were launched between CTD stations. Figure 1 *a* and *b* shows the station location during the cruises in February 2011 and 2010 respectively. The XCTD profiles were quality controlled by following the guidelines in the CSIRO cookbook[21].

The first mode baroclinic radius for the region can be taken as ~30 km (ref. 22). Baroclinic eddies can grow maximum to the size of $2\pi L_r$, where L_r is the Rossby deformation radius[23]. Our sampling interval is roughly 60 km. Hence smallest features that can be identified with the *in situ* measurements will have ~180 km dimension. In this case, even the largest feature, will, however, be resolved only by three data points. To supplement our *in situ* measurements we utilized satellite-derived sea-level anomaly (SLA) maps overlaid by the geostrophic velocities to show the presence of eddies along the cruise track. Geostrophic velocities were downloaded from AVISO (http://www.aviso.oceanobs.com/duacs/). Satellite altimeter SLA data were obtained from AVISO on a 1/3 Mercator grid at 7 day intervals[24]. Contour maps of dynamic height were prepared using the SLA data. From the maps, dynamic heights > 20 cm were considered as anticyclonic eddies and those < –20 cm corresponded with cyclonic eddies. The eddies observed in the study area were visually tracked in order to have an understanding of their time and location of evolution. They were tracked for a period of eight months in the time span ranging from October 2010 to May 2011. The position of the eddy cores was identified from the weekly maps and then the track followed by them was plotted. EKE was calculated by using the formula

$$\mathrm{EKE} = \frac{1}{2}(u^2 + v^2),$$

where u and v are the zonal and meridional geostrophic current anomaly components respectively. Geostrophic velocity anomalies were calculated using the SLA data as follows[25]

$$U = -\frac{g}{f}\left(\frac{\partial \mathrm{SLA}}{\partial y}\right),$$

$$V = -\frac{g}{f}\left(\frac{\partial \mathrm{SLA}}{\partial x}\right),$$

where g is the acceleration due to gravity and f is the Coriolis force.

The sea-surface temperature (SST) data for February 2010 and 2011 were obtained from the Advanced Microwave Scanning Radiometer for the Earth Observing System (AMSRE) version-5 dataset. Maps of Absolute Dynamic Topography (MADT) from CLS/Archiving, Validation and Interpretation of Satellite Oceanographic (AVISO) data was also used to identify the fronts in the study region. Ocean Surface Current Analysis–Realtime (OSCAR; http://www.oscar.noaa.gov) data were used to plot surface ocean currents[26]. The SAM monthly climate mode indices are from the NOAA Climate Prediction Center website (http://www.esrl.noaa.gov/psd/data/climateindices/list).

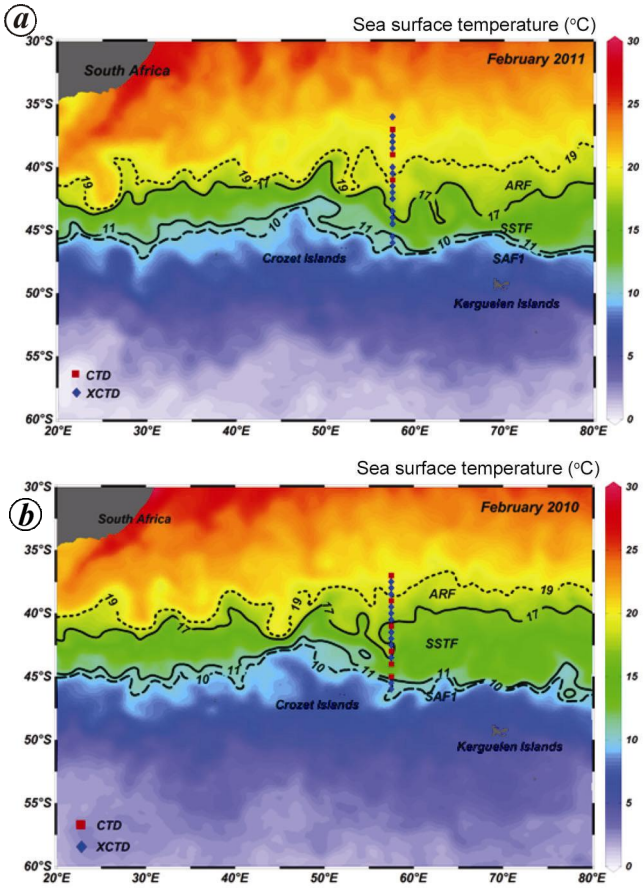

Figure 1. Cruise track overlaid by monthly sea surface temperature (SST) maps. The fronts along the cruise track have been delineated. ***a***, February 2011; ***b***, February 2010.

Results and discussion

Figure 1 *a* and *b* shows the AMSRE monthly averaged SST during February 2011 and 2010. It is clear from the figure that generally in the SO, the temperature gradually decreases southward and at the frontal locations there is a

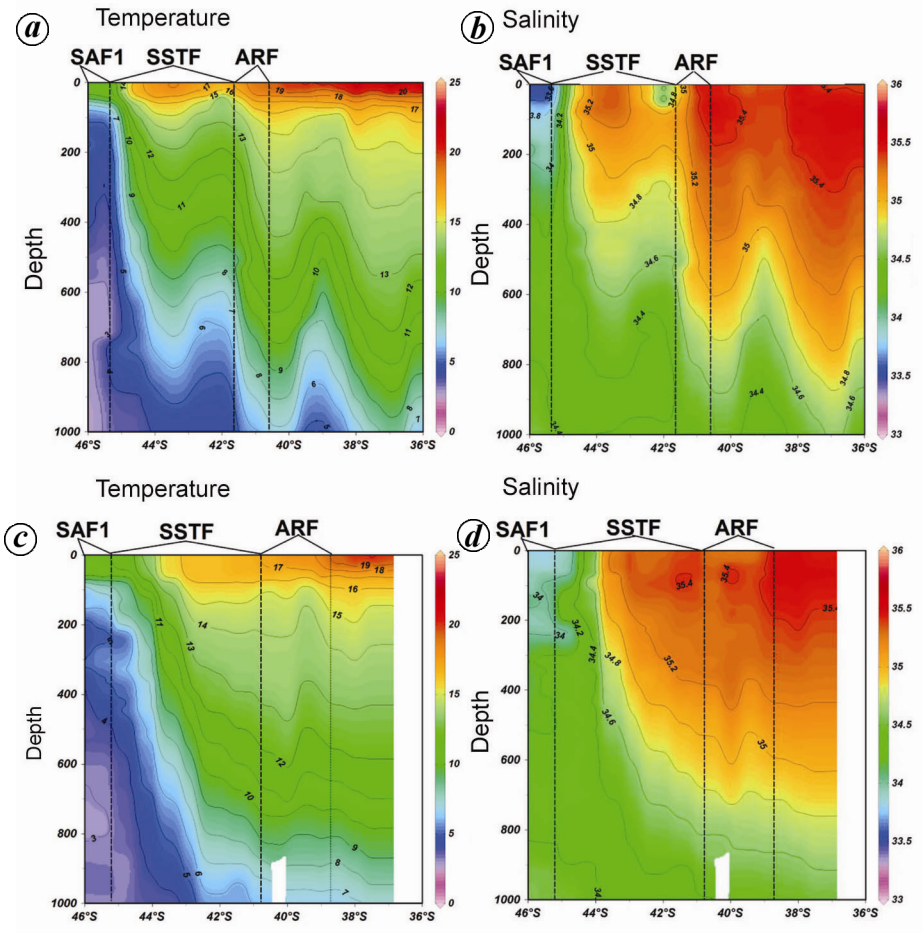

Figure 2. Vertical section of temperature and salinity in (***a***, ***b***) 2011 and (***c***, ***d***) 2010.

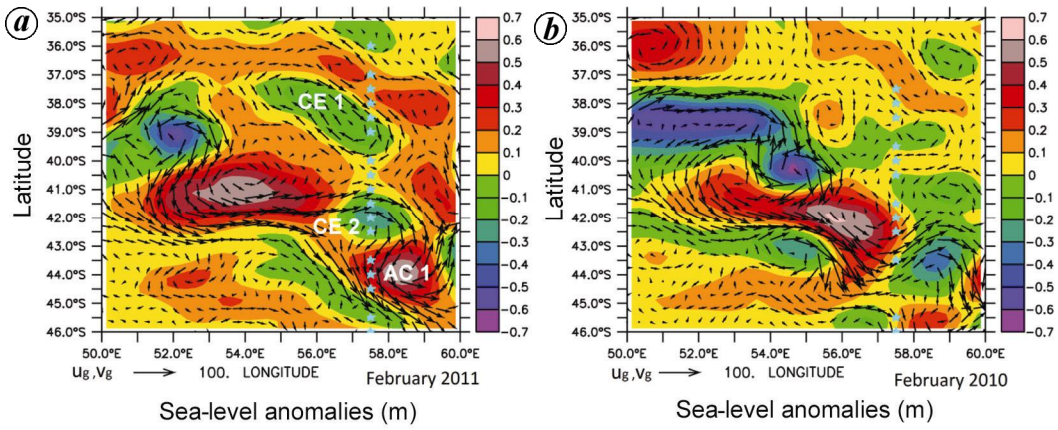

Figure 3. Sea-level anomalies overlaid by the geostrophic velocities over the study area during (***a***) 2011 and (***b***) 2010.

sudden decrease in temperature[27]. The Agulhas Return Front (ARF), Southern Subtropical Front (SSTF), and Subantarctic Front (SAF) are deemed as regions where SST decreases suddenly from 19°C to17°C, 17°C to 11°C and 11°C to 9°C respectively[28–30]. These fronts are highlighted in the Figure 1. From the satellite maps of SST it is clear that the SSTF in 2011 is a narrower front compared to that in 2010. It has been noted in earlier studies that in the western Indian sector of SO, the ARF, SSTF and SAF1 are merged as a single front[30,31]. The thermohaline section shown in Figure 2 suggests that during 2011, the section of temperature (Figure 2 *a*) and salinity (Figure 2 *b*) is characterized by troughs and ridges. However, during 2010 (Figure 2 *c* and *d*) no such features were observed, except for one at 41°S where the isotherm shoaling was noticed, but this was limited to the subsurface levels.

It can also be noted that the undulation in isolines of temperature and salinity during 2011 reached up to 1000 m. These undulations were clearly evident in the 11°C isotherm that shoaled from 600 to 700 m depth at 40.5°S to about 300 m at 42°S. During 2010, the surface temperature gradually decreased from 20°C at 36°S to about 11°C at 46°S (Figure 2 *c*). Salinity varied from 35.4 at 37°S to 33.8° at 46°S (Figure 2 *d*). This gradual variation is in contrast with the north–south variability during 2011, where low SST (17°C) is noted at 42°S and again higher SST (18°C) is noted further south at 44°S. The undulations (troughs and ridges) noted in the thermohaline sections are due to the vertical water column movements. These movements can be associated with Ekman pumping or presence of eddies across the cruise track. To understand the role of eddies along the cruise track, we will further analyse the SLA plots during February 2011 and 2010.

Figure 3 *a* and *b* shows the SLA plots overlaid by the geostrophic velocities during February 2011 and 2010 respectively. The satellite SLA for the observation period of 2011 (Figure 3 *a*) is characterized by two cyclonic (characterized by negative SLA) and one anticyclonic (characterized by positive SLA) circulation pattern centred at 39°S, 42°S and 44°S respectively, which coincides with the locations of the troughs/ridges in the temperature and salinity sections (Figure 2 *a* and *b*). However, the Ekman pumping derived from the ASCAT wind stress curl does not show any correlation with the undulation in the thermohaline section (figure not shown). Hence, it is apparent that the troughs and ridges in the thermohaline structure are the manifestations of cyclonic and anticyclonic eddies. We name these eddies as CE1, CE2 and AC1 located respectively at 39°S, 42°S and 44°S. The hydrographic transect occupied during the survey passes through the centre of CE2 and along edges of CE1 and AC1. The trajectories of the three eddies have been studied for a period of eight months from October 2010 to May 2011 (Figure 4). The cold core eddy CE1 developed in the study area on 17 November 2010. This eddy propagated in a southwesterly direction and was seen at the station location on 2 February 2011, after which it moved westwards. The second cold core eddy CE2 was located at 43°S 57°E on 6 October 2010. CE2 propagated in a northerly direction until 15 December 2010, after which it turned eastward and persisted at the station location for a period of almost 20 days and eventually moved westwards. After 2 March 2011, it was observed that CE2 turned eastward. The warm core eddy AC1 observed at station location 44°S moved in a southwesterly direction from October 2010. From the track followed by AC1 it is evident that this eddy was present near the station location for approximately 8 months. Thus except for CE1, CE2 and AC1 persisted at the station location for at least about 8 months. The track of eddies identified by the visual observations is highlighted in Figure 4. One can also notice from Figure 3 *b* that during February 2010, there were no eddies across the cruise track.

To further understand the vertical thermohaline structure of eddies noted during February 2011, we plotted the profiles of temperature, salinity and density at the eddy stations (Figure 5 *a*–*c*). One of the evident features in the profiles is the fresher and colder water column at the cyclonic eddy observed at 42°S. The profile was characterized by well-developed subsurface temperature minimum layer capped in the upper 100 m by a relatively warm and fresh surface layer. On the other hand, at the anticyclonic eddies the water column was warmer and saltier than the cyclonic eddies. The eddies appear to be density compensated below 200 m.

The water mass analysis using the temperature–salinity (*T*–*S*) plots (Figure 6 *a* and *b*) during 2011 and 2010 showed different water masses in the region. The major water masses in the upper 1000 m noted in the region are Subtropical Surface Waters (STSW), Subantarctic Surface Waters (SASW) and Subtropical Mode Waters (STMW). The STSW originates between 29°S and the Subtropical front at about 40°S (ref. 32). The Subtropical front is the boundary between the warmer and higher, saline STSW and cooler, fresher SASW. STSW is defined by temperature range 15°–24°C and salinity range 35.50–34.60 (ref. 33), and in the Crozet Basin it is characterized by relatively high temperature and salinity (> 12°C, > 35.1)[13]. SASW is defined by the characteristics temperature of

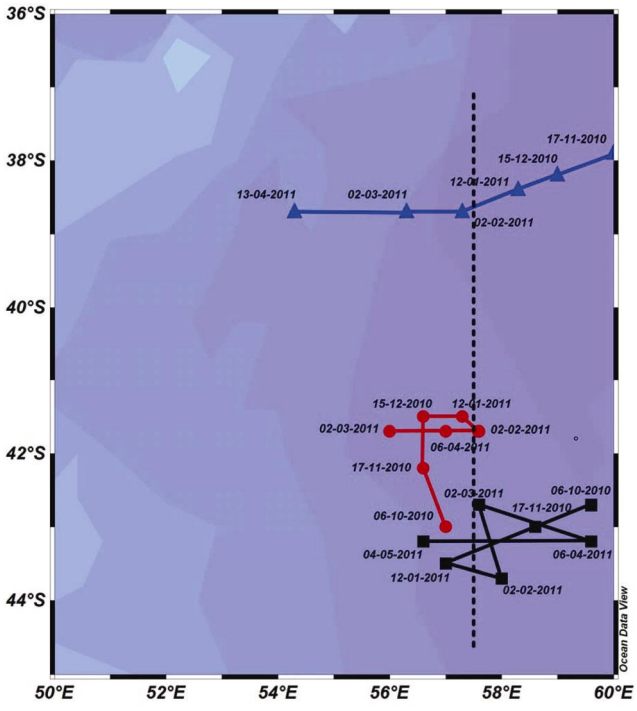

Figure 4. Eddy trajectory showing the movement of the three eddies identified in the study location, CE1 (blue triangle), CE2 (red circle) and AC1 (black square). The black dotted line shows the cruise track along which observations have been carried out.

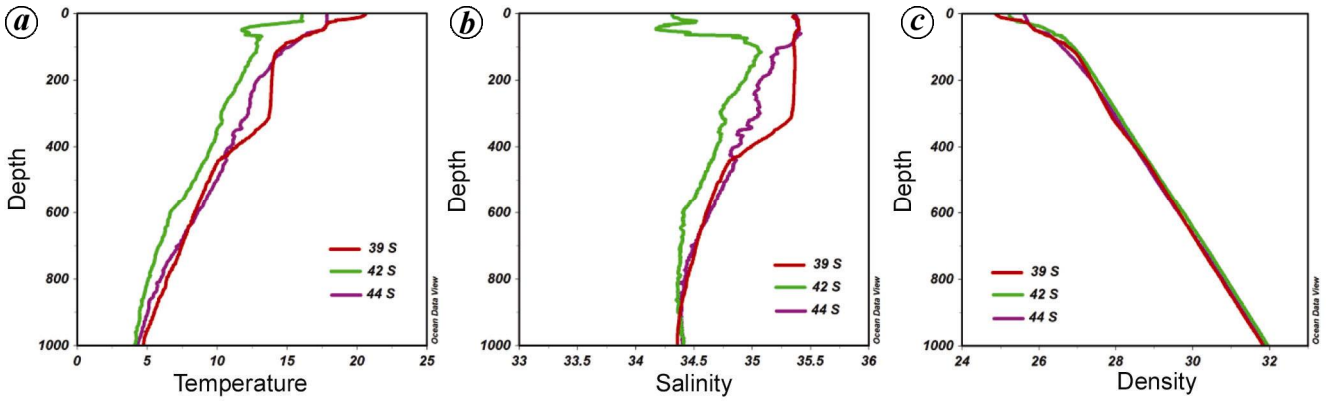

Figure 5. Profiles of (*a*) temperature, (*b*) salinity and (*c*) density at the eddy location during the 2011 expedition.

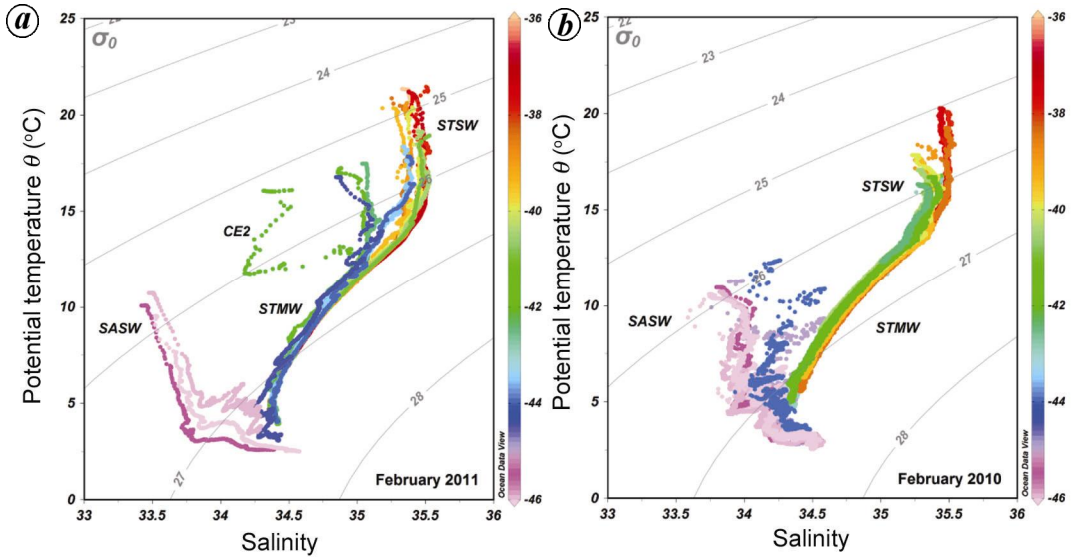

Figure 6. Water masses seen along the cruise track: (*a*) 2011; (*b*) 2010.

around 9°C and salinity < 34. STMW is usually identified in the temperature range 11°–14°C and salinity range 35–35.4. In the present study, the characteristics of STSW provided by Park *et al.*[13] have been considered because the study area is close to the Crozet Basin. *T*–*S* plots for station locations during 2011 show the presence of STSW up to 44°S (Figure 6 *a*), but the presence of this water mass was not noticed at 42°S, where a shoaling of the isolines was noticed in the thermohaline structure. The surface waters at 42°S showed neither *T*–*S* characteristic of STSW nor SASW. Studies along the southwest Indian ridge have shown that surface waters in the eddy regions often get modified either due to air–sea interactions at those latitudes or due to the injection of surface waters from different locations[34]. *T*–*S* plots for 2010 revealed characteristics of STSW up to 42°S (Figure 6 *b*). At 44°S, where signatures of STSW were noticed during 2011, temperature was in the range 2.5–12°C and salinity in the range 34–34.5. Thus, it is apparent that during 2011 the southward extent of the STSW was till 44°S, whereas during 2010 STSW was confined only to the source region. The increased southward presence of STSW during February 2011 compared to that of 2010 can be mediated by eddies in the region.

The eddies noted in the study area are associated with highly dynamic ARC flowing from the southern tip of Africa to the east up to 80°E (ref. 35, 36). This is a part of the Agulhas Current which loops and returns eastward off the coast of southern Africa. This current flows parallel or is juxtaposed to the Subtropical front[37]. Due to the presence of ARC which is dynamically unstable, STF in the SO is characterized by high mesoscale turbulence[33]. Figure 7 *a* and *b* shows the EKE distribution during February 2011 and 2010 respectively. The most evident feature in the figure is the high EKE patch and its southward meandering noted east of 50°E. Figure 7 *c* and *d* shows the OSCAR currents during 2011 and 2010 respectively. From the figure it is clear that the high EKE patch

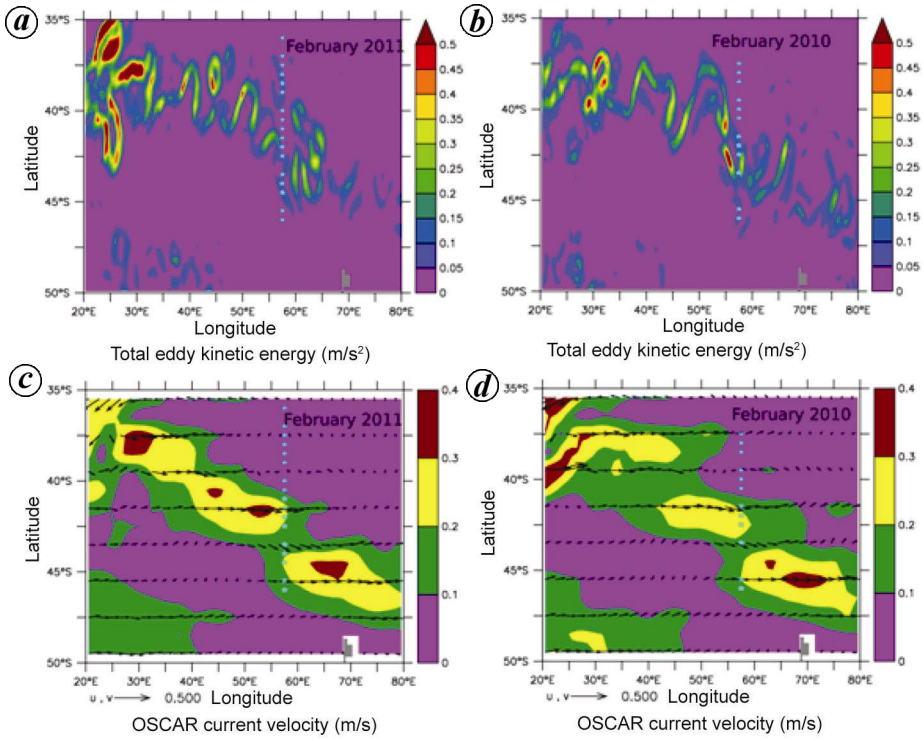

Figure 7. Eddy kinetic energy (EKE) maps over the study area during February (***a***) 2011 and (***b***) 2010. OSCAR currents over the study area during February (***c***) 2011 and (***d***) 2010.

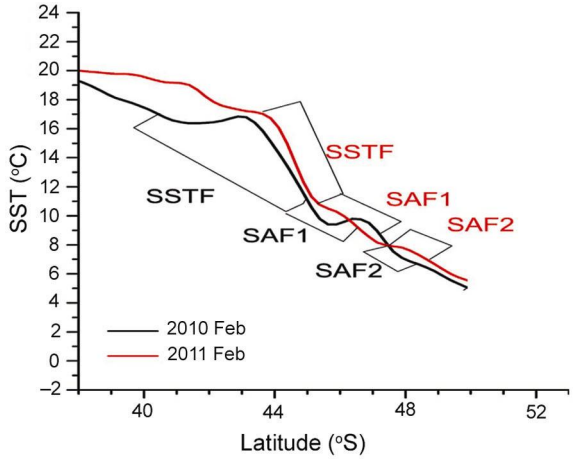

Figure 8. Maps of Absolute Dynamic Topography profiles showing the frontal extend during 2011 and 2010.

is associated with the ARC. Previous studies[29,30] suggested that according to the meandering of the ARC, the fronts shift southward and hence the presence of STSW can be noted further south. The meandering of the ARC is mainly attributed to the presence of bottom topographic features[38]. The presence of southward extension of STSW during February 2011 can be attributed to the southward meandering of the ARC. As the ARC passes from shallow topographic features in the west to deep ocean bottom eastern region to maintain the potential vorticity, the current meanders southward. However, satellite-derived frontal location based on satellite SST averaged over February 2010 and 2011 along 57.5°E clearly suggests that the SSTF location is slightly different between February 2010 and 2011 (Figure 8). These observations invite a detailed interpretation of the presence of STSW further south during 2011.

It is clear from the satellite pictures that the large-scale circulation pattern and frontal locations are different during February 2011 and 2010. It indicates that meandering of the ARC and individual eddies which are pinched off from the core of the ARC can transport STSW further southward. The presence of eddies is evident from the undulations of isotherms during the cruises. The station locations are on the eastward edge of CE1, at the centre of CE2 and at the westward edge of the anticyclonic eddy AC1. Eastward and westward edges of the cyclonic and anticyclonic eddies respectively, are characterized by southward flow that transports the warm high saline subtropical surface waters to the south. *T*–*S* plots for the station locations (Figure 6 *a*) reveal that along the peripheries of the eddies water mass characteristics are intact, whereas in the interior of the eddies the water mass characteristics are modified. This shows that peripheries of the eddies promote unaltered southward transport of the STSW (Figure 9). At the centre of the cyclonic eddy, water masses are modified as seen in the *T*–*S* plots from the stations (Figure 6 *a*). STSW could not be traced south of 45°S. Also, 45°S was characterized by sharp gradients in temperature and salinity, marking the SAF. When STSW

reached 45°S, it might have either subducted or transported eastward by the ACC. During 2010, even though the meandering of the ARC was not significantly different, the absence of eddies (Figure 3 *b*) along the hydrographic transect could have reduced the southward transport of the STSW. We do not notice this transport for deeper water masses. Evolution of eddies encountered during 2011 showed they are persistent features of the region at least for 8 months. Persistence of these eddies for about 8 months indicates a large transport of STSW towards SAF. When compared to 2010, 2011 was characterized by more eddies. This, however, could be a chance occurrence, since our survey was one time spot measurements and may not reflect the large-scale interannual variability of eddy characteristics in the region.

An estimate of the eddy-induced transport was carried out by noting the width of the maximum transport along the southward flowing limb of the AC1 and average velocity along that width. This was then multiplied with the depth of mixed layer in which the STSW can be found. The estimated amount is close to about 0.44 Sv towards the SAF. Persistence of these eddies for about 8 months indicates a large transport of STSW towards SAF during years of increased EKE. The negative trend of v component of geostrophic velocity (v_{geo}; Figure 10 *a*) obtained in the present study implies an increase in southward movement of the water masses. A coarse-resolution climate modelling study[39] has demonstrated that enhanced mesoscale eddy activity, following an increase in the wind stress, increases the poleward heat transport. Our analysis also supports these observations by the more southerly presence of STSW in 2011.

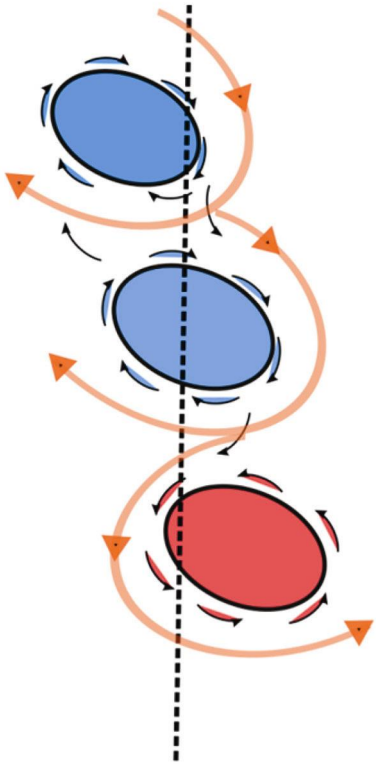

Figure 9. Schematic diagram showing the path of subtropical surface water (thick orange line) facilitated by the eddies present.

In order to gain insight into this interannual variability and to investigate whether one time measurements reflect large-scale processes, we computed the EKE averaged over a box (40–80°E, 35–45°S) in the Indian sector of the SO (Figure 10 *b*). EKE is characterized by an increasing trend with a biennial variability. It is evident from the plot that EKE was low during 2010 and reached a maximum during 2011. Thus the difference in the number of eddies we noted during 2010 and 2011 is a basin wide characteristic. Hence large-scale processes may be involved in the realization of observed variability in the thermohaline structure and water masses.

In SO, interannual variability in EKE may result from changes in SAM. In an analysis of oceanic EKE and changes in SAM[2], it was observed that EKE and SAM are characterized by a 2–3 year lag, especially for the Indian Ocean sector. In our case the lag is ~1 year, somewhat faster than expected (Figure 10 *c*). To explore the EKE–SAM relationship an eddy-resolving quasi-geostrophic model was also used[2]. The model results varied under different scenarios. For standard perturbation of a wind stress of ~0.21 Nm^{-2}, the lag in peak kinetic energy was 1.2–2 years, whereas for a strong perturbation with a wind stress of ~0.25 Nm^{-2}, the lag was found to be ~1 year. Thus the fast response we observed could be due to a strong perturbation in the wind fields. This increase in EKE was associated with the increase in the circumpolar wind stress and the lag is due to the time taken to influence the circulation in the deep ocean[2]. Thus the observed interannual variability in the thermohaline structure and the water mass is a result of large-scale variability arising from changes in annular mode.

Conclusions

Data obtained from expendable probes and CTD during the expedition to SO along 57°30′E during the austral summer 2010 and 2011 were analysed. The analysis revealed that the year-to-year variability in the hydrographic structure was due to the presence of eddies. Troughs and ridges of isotherms and isohalines were dominant in the vertical section of temperature and salinity during 2011. SSHA data clearly indicated the presence of cyclonic and anti-cyclonic eddies along the cruise track. The eddies present in the study area transported STSW southward by means of the enhanced meridional velocities along the peripheries of the eddies. Absence of eddies during 2010 restricted the southward transport of STSW to the region of its origin. Signatures of STSW south of 45°S were not clear. STSW might have either subducted or transported eastward along the SAF. Analysis

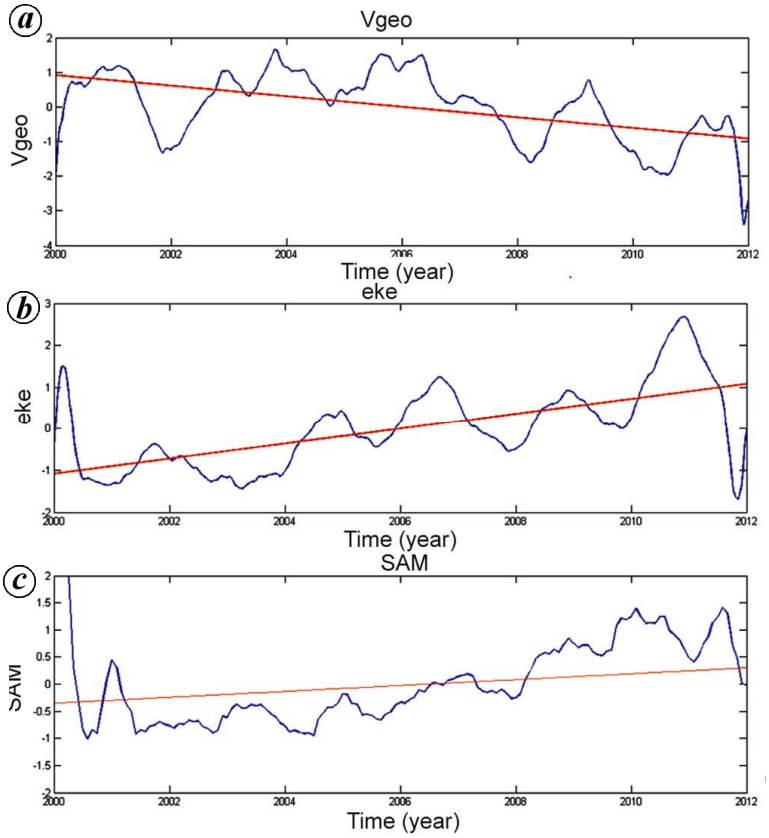

Figure 10. The variation of (***a***) *v* component of geostrophic velocity (v_{geo}); (***b***) Eddy kinetic energy; (***c***) Southern annual mode index.

of EKE shows that it peaks a year after the peak value in the SAM, suggesting the role of large-scale variability in controlling the EKE. Positive linear trend in the EKE suggests more southward transport of subtropical water masses which will have implications on the SO vertical mixing, air–sea interaction, sea-ice and water mass formation.

1. Farneti, R., Delworth, T. L., Rosati, A. J., Griffies, S. M. and Zeng, F., The role of mesoscale eddies in the rectification of the Southern Ocean response to climate change. *J. Phys. Oceanogr.*, 2010, **40**, 1539–1557.
2. Meredith, M. P. and Hogg, A. M., Circumpolar response of Southern Ocean eddy activity to a change in the Southern Annular Mode. *Geophys. Res. Lett.*, 2006, **33**, L16608.
3. Hughes, C. W., Meredith, M. P. and Heywood, K. J., Wind-driven transport fluctuations through Drake Passage: a southern mode. *J. Phys. Oceanogr.*, 1999, **29**, 1971–1992.
4. Gille, S. T., Stevens, D. P., Tokmakian, R. T. and Heywood, K. J., Antarctic Circumpolar Current response to zonally averaged winds. *J. Geophys. Res.*, 2001, **106**, 2743–2759.
5. Hogg, A. and Blundell, J. R., Interdecadal variability of the Southern Ocean. *J. Phys. Ocean.*, 2006, **36**, 1626–1645.
6. Dijkstra, H. A. and Ghil, M., Low-frequency variability of the large-scale ocean circulation: a dynamical systems approach. *Rev. Geophys.*, 2005, **43**, RG3002; doi: 10.1029/2002RG000122.
7. Sheen, K. L. *et al.*, Eddy-induced variability in Southern Ocean abyssal mixing on climatic timescales. *Nature Geosci.*, 2014, **7**, 577–582; doi: 10.1038/ngeo2200.
8. Morrow, R., Ward, M. L., Hogg, A. M. and Pasquet, S., Eddy response to Southern Ocean climate modes. *J. Geophys. Res.*, 2010, **115**, C10030.
9. Colton, M. T. and Chase, R. P., Interaction of the Antarctic Circumpolar Current with bottom topography: an investigation using satellite altimetry. *J. Geophys. Res.*, 1983, **88**, 1825–1843.
10. Hofmann, E. E., The large-scale horizontal structure of the Antarctic Circumpolar Current from FGGE drifters. *J. Geophys. Res.*, 1985, **90**, 7087–7097.
11. Craneguy, P. and Park, Y. H., Topographic control of the Antarctic Circumpolar Current in the South Indian Ocean. *C. R. Acad. Sci. Paris*, 1999, **328**, 583–589.
12. Lutjeharms, J. R. E. and Baker, D. J., A statistical analysis of the meso-scale dynamics of the Southern Ocean. *Deep-Sea Res.*, 1980, **27**, 145–159.
13. Park, Y.-H., Gamberoni, L. and Charriaud, E., Frontal structure, water masses, and circulation in the Crozet Basin. *J. Geophys. Res.*, 1993, **98**, 12361–12385.
14. Trathan, P. N., Brandon, M. A. and Murphy, E. J., Characterization of the Antarctic Polar Frontal Zone to the north of South Georgia in summer 1994. *J. Geophys. Res.*, 1997, **102**, 10483–10497.
15. Hogg, A., Meredith, M. P., Blundell, J. R. and Wilson, C., Eddy heat flux in the Southern Ocean: response to variable wind forcing. *J. Climate*, 2008, **21**, 608–620.
16. de Szoeke, R. A. and Levine, M. D., The advective flux of heat by mean geostrophic motions in the Southern Ocean. *Deep Sea Res., Part-I*, 1981, **28**, 1057–1085.
17. Lee, M. M., George Nurser, A. J., Coward, A. C. and de Cuevas, B. A., Eddy advective and diffusive transports of heat and salt in the Southern Ocean. *J. Phys. Oceanogr.*, 2007, **37**, 1376–1393.

18. Arhan, M., Speich, S., Messager, C., Dencausse, G., Fine, R. and Boye, M., Anticyclonic and cyclonic eddies of subtropical origin in the subantarctic zone south of Africa. *J. Geophys. Res*., 2011, **116**(C11004), doi: 10.1029/2011JC007140.
19. Park, Y. H., Gamberoni, L. and Charriaud, E., Frontal structure, transport and variability of the Antarctic Circumpolar Current in the South Indian Ocean sector, 401–801E. *Mar. Chem.*, 1991, **35**, 45–62.
20. Lutjeharms, J. R. E. and Valentine, H. R., Eddies at the subtropical convergence south of Africa. *J. Phys. Oceanogr*., 1988, **18**, 761–774.
21. Bailey, R., Gronell, A., Phillips, H., Tanner, E. and Meyers, G., Quality control cookbook for XBT data, Version 1.1. CSIRO Marine Laboratories Reports, 1994, p. 221.
22. Chelton, D. B., deSzoeke, R. A., Schlax, M. G., El Naggar, K., and Siwertz, N., Geographical variability of the first-baroclinic Rossby radius of deformation. *J. Phys. Oceanogr*., 1998, **28**, 433–460.
23. Kamenkovich, V. M., Koshlyakov, M. N. and Monin, A. S. (eds), *Synoptic Eddies in the Ocean*, Reidel, Dordrecht, Holland, 1986, p. 433.
24. Ducet, N., Le Traon, P. Y. and Reverdin, G., Global high resolution mapping of ocean circulation from TOPEX/POSEIDON and ERS-1/2. *J. Geophys. Res*., 2000, **105**, 19477–19498.
25. Pond, S. and Pickard, G. L., *Introductory Dynamic Oceanography*, Pergamon Press, New York, 1978.
26. Bonjean, F. and Lagerloef, G. S. E., Diagnostic model and analysis of the surface currents in the tropical Pacific Ocean. *J. Phys. Oceanogr.*, 2002, **32**, 2938–2954.
27. Deacon, G. E. R., The hydrology of the Southern Ocean. *Discov. Rep.*, 1937, 15-122.
28. Belkin, I. M. and Gordon, L., A Southern Ocean fronts from the Greenwich meridian to Tasmania. *J. Geophys. Res*., 1996, **101**, 3675–3696.
29. Holliday, N. P. and Reed, J. F., Surface oceanic fronts between Africa and Antarctica. *Deep Sea Res.*, *Part-I*, 1998, **45**, 217–238.
30. Anilkumar, N., Jenson, G. V., Chacko, R., Murukesh, N. and Sabu, P., Variability of fronts, freshwater input and chlorophyll in the Indian Ocean sector of the Southern Ocean. *N.Z. J. Mar. Freshwater Res*. (in press); doi: 10.1080/00288330.2014.924972.
31. Anilkumar, N. *et al.*, Fronts, water masses, and heat content variability in the western Indian sector of the Southern Ocean during austral summer 2004. *J. Mar. Syst*., 2006, **63**, 20–34.
32. Read, J. F. and Pollard, R. T., Structure and transport of the Antarctic Circumpolar Current and Agulhas Return Current at 401E. *J. Geophys. Res*., 1993, **98**, 12281–12295.
33. Darbyshire, M., The surface waters near the coasts of southern Africa. *Deep-Sea Res*., 1966, **13**, 57–81.
34. Ansorge, I. J. and Lutjeharms, J. R. E., Direct observations of eddy turbulence at a ridge in the Southern Ocean. *Geophys. Res. Lett*., 2005, **32**, doi: 10.1029/2005GL022588.
35. Read, J. F., Lucas, M. I., Holley, S. E. and Pollard, R. T., Phytoplankton, nutrients and hydrography in the frontal zone between the southwest Indian subtropical gyre and the Southern Ocean. *Deep Sea Res.*, *Part I*, 2000, **47**(12), 2341–2367; http://dx.doi.org/10.1016/S0967-0637(00)00021-2.
36. Beal, L. M., Ruijter, W. P., Biastoch, A. and Zahn, R., On the role of the Agulhas system in ocean circulation and climate. *Nature*, 2011, **472**, 429–436.
37. Lutjeharms, J. R. E. and Ansorge, I. J., The Agulhas Return Current. *J. Mar. Syst.*, 2001, **30**, 115–138.
38. Nuncio, M., Luis, A. J. and Yuan, X., Topographic meandering of Antarctic Circumpolar Current and Antarctic Circumpolar Wave in the ice–ocean–atmosphere system. *Geophys. Res. Lett.*, 2011, **38**, L13708; doi:10.1029/2011GL046898.
39. Fyfe, J., Saenko, O., Zickfeld, K., Eby, M. and Weaver, A., The role of poleward intensifying winds on Southern Ocean warming. *J. Climate*, 2007, **20**, 5391–5400; doi: 10.1175/2007jcli1764.1.

ACKNOWLEDGEMENTS. This work was supported by the Ministry of Earth Sciences, Government of India. We thank the Director, NCAOR, Goa for support and encouragement. We also thank the cruise participants and staff at NCAOR for help in the implementation and completion of this study. This is NCAOR contribution number 21/2014.

Received 21 January 2014; revised accepted 9 August 2014